

Journal of Materials Chemistry A

Accepted Manuscript



This is an *Accepted Manuscript*, which has been through the Royal Society of Chemistry peer review process and has been accepted for publication.

Accepted Manuscripts are published online shortly after acceptance, before technical editing, formatting and proof reading. Using this free service, authors can make their results available to the community, in citable form, before we publish the edited article. We will replace this *Accepted Manuscript* with the edited and formatted *Advance Article* as soon as it is available.

You can find more information about *Accepted Manuscripts* in the [Information for Authors](#).

Please note that technical editing may introduce minor changes to the text and/or graphics, which may alter content. The journal's standard [Terms & Conditions](#) and the [Ethical guidelines](#) still apply. In no event shall the Royal Society of Chemistry be held responsible for any errors or omissions in this *Accepted Manuscript* or any consequences arising from the use of any information it contains.

Guest-dependent thermochromic feature in metal-organic framework and its thin film on different supports

Ping-Chun Guo,^{a, b} Tian-Yu Chen,^{a, b} Xiao-Ming Ren,^{*a, b} Zhenyu Chu,^a Wanqin Jin^{*a}

^aState Key Laboratory of Materials-Oriented Chemical Engineering, Nanjing University of Technology, Nanjing 210009, P.R. China

^bCollege of Science, Nanjing University of Technology, Nanjing 210009, P. R. China

Tel.: +86 25 58139476

Fax: +86 25 58139481

E-mail: xmren@njut.edu.cn (X.M.R.) and wqjin@njut.edu.cn (W.Q.J.)

Abstract

A three-dimensional NbO-type metal-organic framework (MOF) is composed of paddle-wheel-type dinuclear Cu_2 secondary units and 1, 1'-ethynebenzene-3, 3', 5, 5'-tetracarboxylate (EBTC^{4-}) linkers. Two types of nanometer-sized cavities are formed in this framework with ca. 8.5 Å in diameter for small one and a dimensional of ca. 8.5×21.5 Å for the larger and irregular elongated cavity. The guest molecules, H_2O , DMF and DMSO, occupy in the cavities of the as-prepared MOF crystal (labeled as MOF **1**). MOF **2** was obtained by guest-exchange approach using CH_3OH , and the H_2O and CH_3OH molecules reside in the cavities of **2**. Two MOFs show greenish-turquoise color at ambient temperature due to the d-d transition of Cu^{2+} ion in the framework, and the reversible thermochromic behavior owing to the change of coordination environment of Cu^{2+} ion with varying temperature. The films of **1** and **2** were fabricated on the $\alpha\text{-Al}_2\text{O}_3$ and SiO_2 supports by seeded growth method, displaying similar reversible thermochromic behavior to the corresponding MOFs. This study suggested the possibility of novel thermochromic materials in the rational design MOFs.

Keywords: Cu-MOF, **1**, 1'-ethynebenzene-3,3',5,5'-tetracarboxylate, thin film, thermochromism

Introduction

The color of a thermochromic material is sensitive to the temperature; such a material has many technological applications in the fields, such as smart windows which have been used to improve the solar energy efficiency of the houses and vehicles and hence to the reduction of energy consumption and CO₂ emission,¹ temperature sensors,² color filters³ and displays.⁴ Most of the thermochromic materials, up to date, are still traditional inorganic oxides, sulfides or halides, for instance, VO₂,⁵ Ag₂S,⁶ Cu₂HgI₄,⁷ Ag₂HgI₄⁸ as well as nematic mesophase liquid crystal⁹ and poly(phenylenevinylene)-based polymers.¹⁰ In this context, the studies of the thermochromic nature on metal-organic frameworks-based (MOFs) coordination polymers, to the best of our knowledge, have remained sparse, even if some mononuclear transition metal complexes, bis(dimethylammonium)-tetrachloronickelate,¹¹ bis(diethylammonium)tetrachlorocuprate¹² and Cu(acac)₂¹³ have been known to show the thermochromic behavior.

MOFs are a class of crystalline hybrid materials formed by the connection of metal centers or clusters and organic linkers.¹⁴ The porous MOFs-based materials have potential applications in a wide range of fields, for instance, gas-sorption,¹⁵ enantioselective recognition and separation,¹⁶ catalytic,¹⁷ magnetic,¹⁸ and electrical (or dielectric)¹⁹ properties. This is due to their designable and controllable porosity, extremely large specific surface area, structural variety and modifiable surface chemical and physical natures of the pores. MOFs with designable structure and desirable property are also the good candidates in thermochromic materials; this is because (1) the d-d transition of transition metal ion in a coordination compound falls within the visible spectroscopy region and the wavelength of d-d transition band is related strongly to the crystal field nature of transition metal ion coordination sphere, as a result, to modify the coordination environment of a transition metal ion, which is easily achievable in the porous MOFs, may change the spectroscopy feature of d-d transition band. (2) MOFs tend to display rich structural polymorphism, the different polymorphs, generally, show distinct electric structures and UV-visible spectra.

Moreover, the single crystal-to-single crystal transformation between different polymorphs is accessible under external stimuli, such as irradiation or temperature change.²⁰

On the other hand, the processing of MOF as film is necessary for a variety of practical applications, and this field has only recently been initiated and is one of the challenges for the development of many special functional devices. To grow the MOF thin films, a number of interesting methods have been employed, including the direct growth/deposition from solvothermal mother solutions,²¹ the secondary growth on seeding layers,²² the stepwise layer-by-layer growth,²³ the electrochemical deposition,²⁴ the combination of Langmuir-Blodgett and layer-by-layer method,²⁵ the stepwise dosing metal salt precursor solution and followed by organic ligand solution²⁶ to assembly MOF nanocrystalline film.²⁷ It is worth noting that the secondary growth method becomes more popular one for growing polycrystalline films due to the low heterogeneous nucleation density of polycrystalline MOF.

In the context of study of MOFs-based materials, we discovered that the copper(II) oxygen clusters MOFs, namely, $\text{Cu}_2(\text{EBTC})(\text{H}_2\text{O})_2\cdot[\text{G}]$ (EBTC = 1, 1'-ethynebenzene-3, 3', 5, 5'-tetracarboxylate; G = guest molecules and represent DMF, DMSO, H_2O or CH_3OH) show the thermochromic property. In this paper, we present the thin film fabrications of the thermochromic MOFs on $\alpha\text{-Al}_2\text{O}_3$ and SiO_2 supports using the secondary growth and the investigation of the fascinating thermochromic properties of both polycrystalline samples and thin films.

Experimental section

Chemical materials

1, 1'-ethynebenzene-3, 3', 5, 5'-tetracarboxylic acid (H_4EBTC) was prepared according the published procedure in literature.²⁸ $\text{Cu}(\text{NO}_3)_2\cdot 3\text{H}_2\text{O}$ (Fluka, 98%), $\text{Cu}(\text{CH}_3\text{COO})_2\cdot \text{H}_2\text{O}$ (Shanghai Sinpeuo Fine Chemical Co., Ltd., 99%) and (3-glycidyloxypropyl)trimethoxysilane (Sigma-Aldrich) were used without further purification. DMF, DMSO and CH_3OH with A. R. grade were directly employed as

solvents. SiO₂ slides, with an area of 10 mm × 10 mm, were purchased from a Chinese company.

Preparation of Al₂O₃ supports

Al₂O₃ supports: Al₂O₃ powders with an average particle size of ca. 0.3-0.4 μm were uniaxially pressed under 8 MPa to prepare into disks with a diameter of 16 mm and thickness of 2 mm. The disks were then sintered at 1200 °C for 2 h to form porous supports with the normal pore size of ca. 110 nm and the porosity of about 35%. One surface of Al₂O₃ disk was polished using 1200-mesh SiC sandpaper, and in turn washed by deionized water and dried under vacuum.

Hydroxyl terminated SiO₂ supports

SiO₂ supports (with an area of 10 mm × 10 mm) were cleaned by immersion in a “piranha” solution, which was prepared using 98% concentrated H₂SO₄ and 30% H₂O₂ in a volume ratio of 3:1 at 100 °C for 1 h. The supports were washed with sufficient amount of deionized water and dried under N₂ stream at ambient temperature. The cleaned surfaces of SiO₂ supports were modified using a 2% solution of (3-glycidyloxypropyl)trimethoxysilane in toluene over night at 70 °C, followed by rinsing with toluene and water, such a treatment was repeatedly performed three times, and then dried at 70 °C. The above-mentioned procedure gave the self-assembly-monolayer (SAM) functionalized SiO₂ supports.

Synthesis of MOF samples

Cu₂(EBTC)(H₂O)₂·[G] (**1**) (G = guest molecules and represent DMF, DMSO and H₂O) was prepared following the published procedure in literature,²⁹ and the phase purity was inspected using powder X-ray diffraction (PXRD) technique. Crystalline sample **1** was treated three times with sufficient CH₃OH (by soaking **1** in CH₃OH) refreshed every 24 h to give [Cu₂(EBTC)(H₂O)₂]_x·[(H₂O)_x(CH₃OH)_y]_∞ (**2**).

Deposition of **1** seeds on different supports

The polished surface of porous alumina disk was, in sequence, (a) dipped in 1 mM H₄EBTC solution of DMF/DMSO (V/V = 1:1) for 30 min, (b) washed with the DMF/DMSO (V/V = 1:1) mixed solvent, (c) dipped in 1 mM Cu(CH₃COO)₂·H₂O solution of DMF/DMSO (V/V = 1:1) for 20 min, and (d) washed with the DMF/DMSO (V/V = 1:1) mixed solvent. The process from step (a) to (d) was repeatedly performed 5 times, and then dried at 50 °C under vacuum for 30 min to give the seeded Al₂O₃ supports.

The SAM-functionalized SiO₂ supports with seeded layers were prepared using the above-mentioned approach, alternative deposition of H₄EBTC and Cu(CH₃COO)₂·H₂O in DMF/DMSO mixed solution for 5 times, to give the seeded SAM-functionalized SiO₂ support. The dried SAM-functionalized SiO₂ supports were used for further preparation of thermochromic MOF films and a range of physical characterizations.

Preparation of MOF films

H₄EBTC (17.7 mg, 0.05 mmol) and Cu(NO₃)₂·3H₂O (53.3 mg, 0.22 mmol) were dissolved in DMF (2 mL) together with DMSO (2 mL). The mixture was stirred for 10 min at ambient temperature and poured into a 25 mL Teflon-lined autoclave, where the seeded Al₂O₃ support was fixed to let its polished surface down towards the autoclave bottom. The autoclave was cooled to ambient temperature with a cooling rate of 20 °C·h⁻¹ after crystallization at 65 °C over 24 h. The as-prepared **1**/Al₂O₃ film were cleaned with DMF/DMSO (V/V = 1:1) and dried at 25 °C under vacuum over 12 h for other uses. The **2**/Al₂O₃ film was obtained by soaking **1**/Al₂O₃ in methanol for 24 h and cleaning by methanol several times, and then drying at ambient temperature.

The same procedure was used to fabricate **1** film on the SAM-functionalized SiO₂ support with seeds (**1**/SiO₂ film). The as-prepared **1**/SiO₂ films were cleaned with DMF/DMSO (v/v = 1:1) and dried at 25 °C under vacuum over 12 h. To soak **1**/SiO₂ in methanol over 24 h, in turn, clean using methanol several times and then dry at ambient temperature to give **2**/SiO₂ film.

Physical measurements

Variable temperature powder X-ray diffraction (PXRD) data were collected on a Bruker D8 diffractometer with Cu K α radiation ($\lambda = 1.5418 \text{ \AA}$) in the temperature ranges 25-230 °C. Thermogravimetric (TG) experiments were performed with STA449 F3 thermogravimetric analyzer in the range 30-700 °C at a warming rate of 10 °C/min under a nitrogen atmosphere and the polycrystalline samples were placed in an Al₂O₃ crucible. Ultraviolet–visible spectroscopy was recorded on Shimadzu UV-2401TC spectrophotometer. The morphologies of solid materials were observed using a Hitachi S-4800 Field Emission Scanning Electron Microscope with gold-coated specimens to increase conductivity. The temperature dependent photographic images were taken at selected temperatures using a Leica DMRX polarizing optical microscope equipped with an LINKAM LTS350 cool and hot stage for the microcrystalline samples and using a digital camera for the MOF films.

Results and discussion

Framework structure and thermal stability of **1**²⁹ and **2**³⁰

1 and **2** crystallize in the rhombohedral space group R-3m with almost the same framework structure.³⁰ As shown in **Figure 1**, the framework is comprised of paddle-wheel-type dinuclear Cu₂ units which are connected through EBTC⁴⁻ ligands to form a three-dimensional (3-D) NbO-type crystal structure, the metal-organic framework possesses two types of nanometer-sized cavities, the small cavity has ca. 8.5 Å in diameter and the larger one shows irregular elongated cavity with a dimensional of about 8.5×8.5×21.5 Å.²⁹ The disordered H₂O, DMF and DMSO guest molecules occupy in two types of cavities of **1**²⁹ and the disordered H₂O and CH₃OH guest molecules are residual in the cavities of **2**. The guest molecules in **1** were removable when the temperature rises up to 230 °C, as well as the H₂O and CH₃OH in **2** are completely removable by heating **2** above 130 °C. The solvent-free MOF is thermally stable below 250 °C at least; this was confirmed by TG (ref. **Figure S1** where the weight losing corresponded to the decomposition of framework appears

above 250 °C) and variable temperature PXRD (ref. **Figure 2**) measurements. As shown in **Figure 2a**, the PXRD profiles at the selected temperatures are almost the same between 25 and 230 °C for **1**; the intensities of most diffraction peaks in PXRD profile above 160 °C reduce while the characteristic diffraction peaks remain up to 200 °C for **2**.

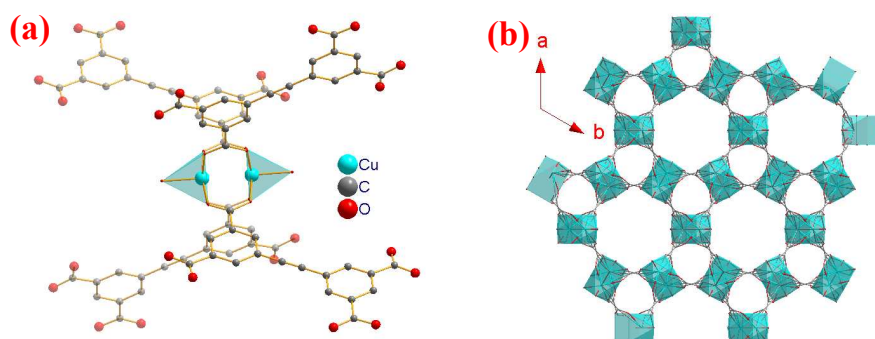


Figure 1 (a) Paddle-wheel-type dinuclear Cu_2 unit and the square pyramid coordination environment of Cu^{2+} ions, which basal plane is comprised of four oxygen atoms from carboxylate groups and the axial site is occupied by H_2O or CH_3OH (b) 3-D NbO-type crystal structure with two types of nanometer-sized cavities in **1** and **2**.

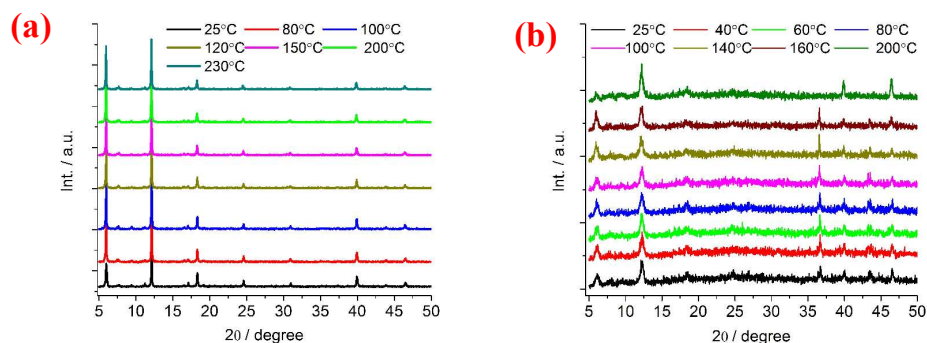


Figure 2 Variable temperature PXRD profiles of (a) **1** and (b) **2**.

Growth of **1** on Al_2O_3 and SAM-functionalized SiO_2 support surfaces

The seeded layer of **1** was fabricated using the alternative deposition of H_4EBTC and $\text{Cu}(\text{CH}_3\text{COO})_2 \cdot \text{H}_2\text{O}$ on the surface of alumina or SAM-functionalized SiO_2 supports. The seed growing processes were repeatedly performed at ambient

temperature. The light-green color originated from **1** becomes progressively obvious with increasing alternative deposition times, and the distinct green-turquoise color was observed on the support surface after alternative deposition 5 times.

The seed growing process of **1** on the surface of α -Al₂O₃ was monitored by PXRD technique and UV-visible spectra, which are shown in Figure 3a and Figure 3b, respectively. It is clear that the intensities of the characteristic reflections, in the 2θ ranges of 5-20°, of **1** and the spectroscopy intensity of d-d transition originated from the coordinated Cu²⁺ ions in **1** increase significantly with increasing the times of alternative deposition of H₄EBTC and Cu(CH₃COO)₂·H₂O.

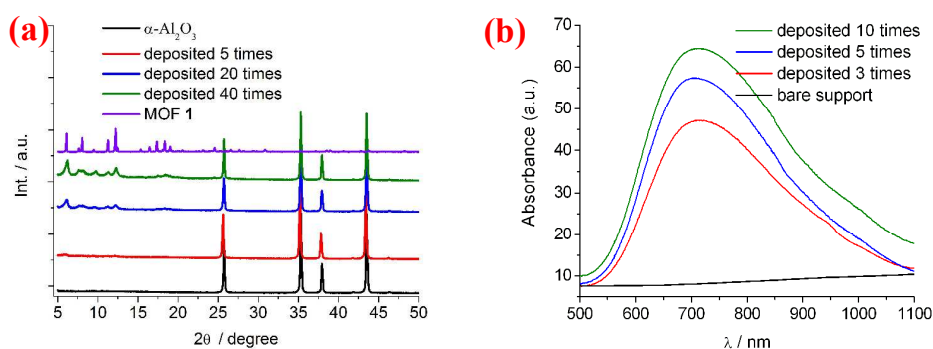


Figure 3 (a) PXRD profiles (b) diffuse-reflectance UV-visible spectra of **1** on alumina support using different alternative deposition times.

The surface morphologies of the polished and the seed growing α -Al₂O₃ supports are shown in Figure 4a and Figure 4b, respectively. It is apparently seen that the seeds layer consists of the aggregate nano-sized particles of **1** on the surface of α -Al₂O₃ support. The PXRD profile of **1**/Al₂O₃ is in good agreement with that of **1** (ref. Figure S2), and absence of other phase besides the α -Al₂O₃ support. Figure 4c shows the surface microstructure of the **1**/Al₂O₃ film, and Figure 4d displays the cross-section of the **1**/Al₂O₃ film, from which it can be found that the film is homogeneous and the thickness of the film is estimated to be ca. 0.5 μ m as well as the film layer is well bonded to the α -Al₂O₃ support. The statistics of particle sizes in the **1**/Al₂O₃ film demonstrate a domain size of crystals around 200 nm from SEM data.

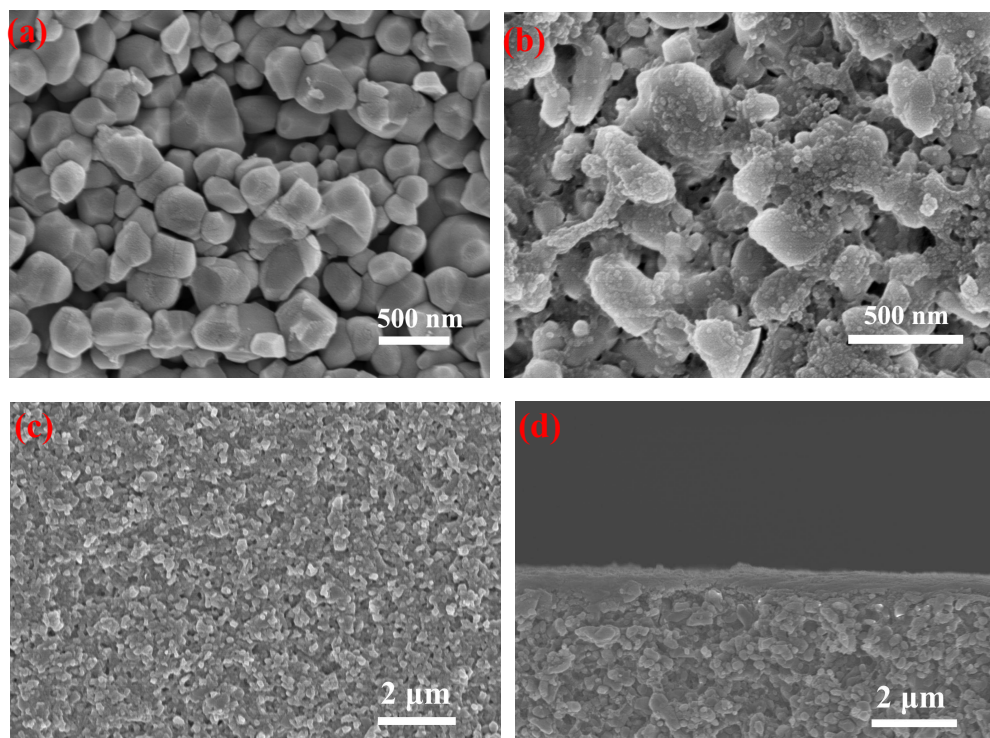


Figure 4 Surface SEM images of (a) polished α - Al_2O_3 support (b) seed layer of **1** on α - Al_2O_3 support (c) surface of the **1**/ Al_2O_3 film (d) cross-section of the **1**/ Al_2O_3 film.

As shown in **Figure 5a**, the nano-sized seeds can be also grown on the surface of SAM-functionalized SiO_2 support. The homogeneous **1**/ SiO_2 film was further fabricated using solvothermal growth approach. **Figure 5b** shows the PXRD patterns of the **1**/ SiO_2 film, SiO_2 support and **1**, which indicates that the crystal structure of film layer on the SAM-functionalized SiO_2 support is consistent with that of **1**. **Figure 5c** and **Figure 5d** display the surface and cross section images of microstructure of the **1**/ SiO_2 . The thickness of the **1**/ SiO_2 film is estimated to be ca. $10\ \mu\text{m}$. The domain size of crystals is estimated to be ca. $200\ \text{nm}$ from SEM data, this particle sizes are comparable to those in the **1**/ Al_2O_3 film.

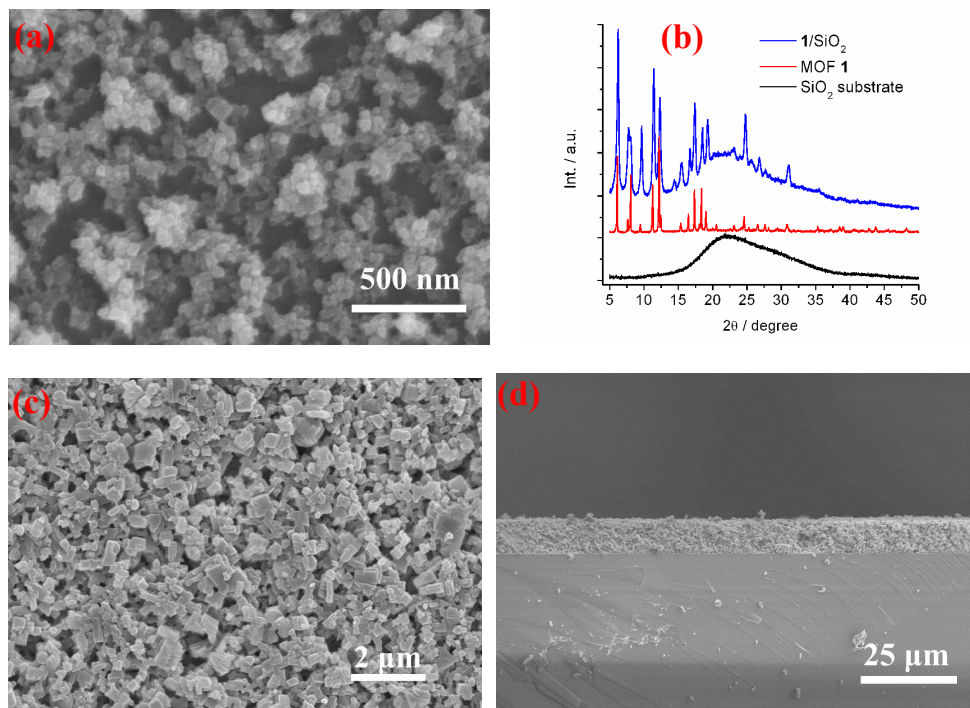


Figure 5 (a) SEM image of seed layer of **1** on the surface of SAM-functionalized SiO₂ support (b) PXRD patterns of SiO₂ support, **1** and **1**/SiO₂ film (c) surface of **1**/SiO₂ film (d) cross-section of **1**/SiO₂ film.

Thermochromic behaviors of crystals and films

The thermochromic behaviors were visually recorded using a polarizing optical microscope for the microcrystalline samples and a digital camera for the films, respectively. **Figure 6-8** show the photos of the crystals and the films of both **1** and **2** at the selected temperatures, and it was found that the crystals of **1** and **2** exhibit quite parallel thermochromic behavior with the corresponding thin films. For example, the colors of crystals **1** and the **1**/Al₂O₃ film were transformed in the order from greenish-turquoise (25 °C) to turquoise (until 140 °C) and light blue (≥ 160 °C) upon heating. In contrast, the thermochromic behavior was observed in the quite lower temperature range for the crystals **2** and **2**/Al₂O₃ film, the color was changed from green-turquoise (25 °C), light blue, and finally navy blue (≥ 60 °C) upon raising temperature. It is worth noting that the temperature dependences of color are fully reversible for both crystals and the corresponding films.

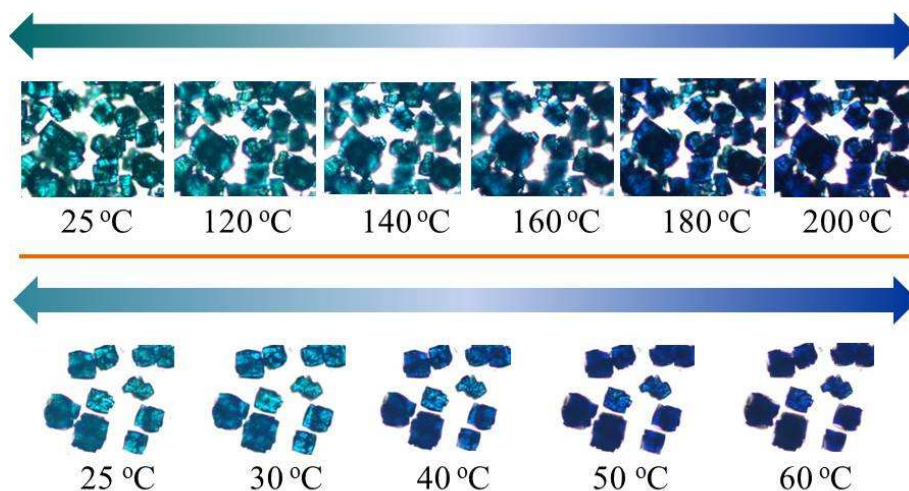


Figure 6 Optical images of **1** (top) and **2** (bottom) at selected temperatures.

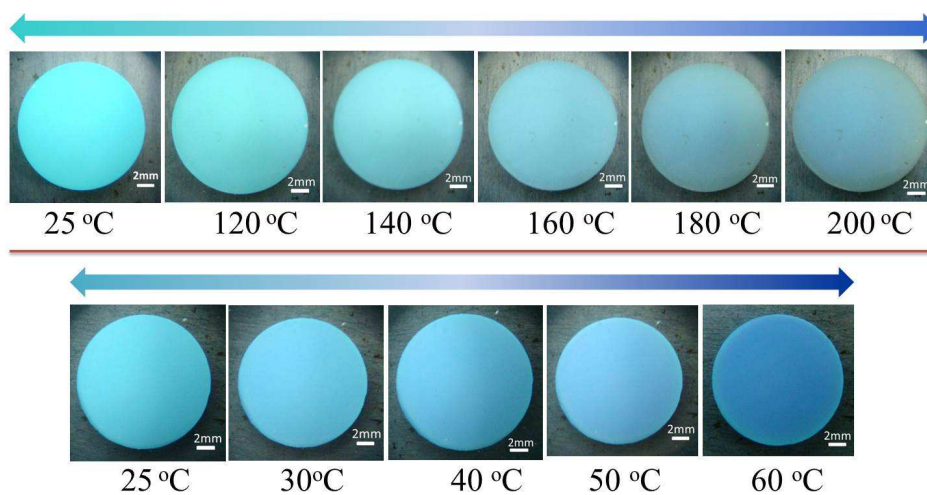


Figure 7 Photographs of $1/\text{Al}_2\text{O}_3$ films (top) and $2/\text{Al}_2\text{O}_3$ (bottom) at different temperatures.

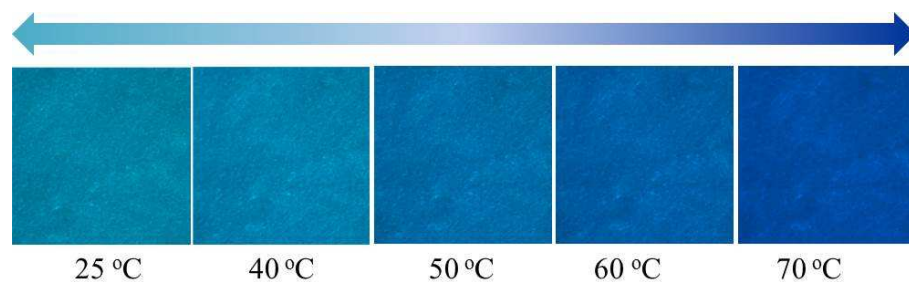


Figure 8 Optical images of $2/\text{SiO}_2$ film with a thickness of $\sim 10 \mu\text{m}$ at selected temperatures.

To understand the origin of thermochromic behavior of these MOFs, we inspected

the temperature dependent PXRD patterns of **1** and **2** at various temperatures. It is hard to see the clear change of the temperature dependent PXRD profiles of **2** owing to the poor signal to noise ratio, while the visible change can be found in the variable temperature PXRD profiles of **1**. As presented in Figure 9, the reflections (2 0 2) and (3 0 3) in **1** shift towards the lower angle side when the temperature is above 150 °C. This result indicates that the expansion of the crystal lattice occurs with increasing temperature in **1**. The lattice expansion probably results in the change of the coordination environment of Cu²⁺ ion (for example, the Cu-O bond distances become longer with increasing temperature, which leads to the change of the crystal field around Cu²⁺ ion), to give the change of d-d transition energy, and this is origin of the thermochromic behavior of **1** and **2**.

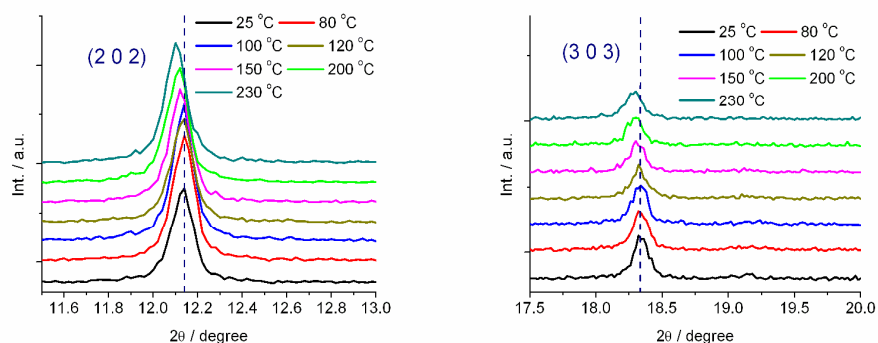


Figure 9 Temperature dependent the reflections (2 0 2) and (3 0 3) at the selected temperatures for **1**.

Conclusion

Two MOFs built from Cu-EBTC framework show 3-D NbO-type crystal structure and reversible thermochromic behavior, and their uniform thin films were fabricated on Al₂O₃ and SiO₂ supports using the seeded growth method. The MOF thin films display similar reversible thermochromic behavior to the corresponding crystals of MOFs. Two MOFs showing greenish-turquoise color at ambient temperature is due to the d-d transition of Cu²⁺ ion in the framework, and the reversible thermochromic behavior of two MOFs originates from the change of coordination environment of Cu²⁺ ions with the varying temperature. This study suggested the possibility of novel

thermochromic materials applied in the fields of thermal sensor and so on through the rational design the structure of MOFs.

The color changes from the greenish-turquoise at 25 °C to the final navy blue when the temperature is above ~160 °C for the crystals and **1** film, while above 60 °C for **2**, this difference is probably related to the distinct ‘chemical pressure’ within the cavities of MOF when there exist different guests, however, the exact reason for such a guest dependent thermochromic behavior is unclear at present stage.

Acknowledgements

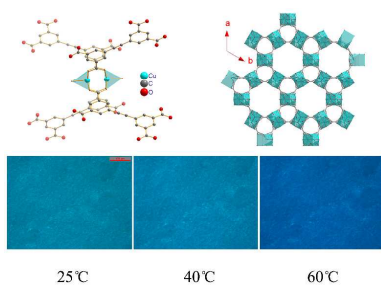
Authors thank the Priority Academic Program Development of Jiangsu Higher Education Institutions, the National Nature Science Foundation of China (Grant no. 91122011, 21271103 and 21176115) and the Innovative Research Team Program by the Ministry of Education of China (No. IRT13070) for financial support.

Notes and references

1. (a) C. G. Granqvist, *Sol. Energy Mater. Sol. Cells*, 2007, **91**, 1529. (b) T. D. Manning, I. P. Parkin, M. E. Pemble, D. Sheel and D. Vernardou, *Chem. Mater.*, 2004, **16**, 74.
2. C. E. Sing, J. Kunzelmann and C. Weder, *J. Mater. Chem.*, 2009, **19**, 104.
3. O. Vigil, C.M. Ruiz, D. Seuret, V. Bermúdez and E. Diéguez, *J. Phys.: Condens. Matter*, 2005, **17**, 6377.
4. (a) L. Y. Liu, S. L. Peng, W. J. Wen and P. Sheng, *Appl. Phys. Lett.* 2007, **90**, 213508. (b) J. Livage, *Coord. Chem. Rev.*, 1999, **190–192**, 391.
5. (a) M. Zhou, J. Bao, M.S Tao, R. Zhu, Y. T. Lin, X.D. Zhang and Y. Xie, *Chem. Commun.*, 2013, **49**, 6021. (b) T. D. Manning, I.P. Parkin, M.E. Pemble, D. Sheel and D. Vernardou, *Chem. Mater.*, 2004, **16**, 744.
6. M. H. Hebb, *J. Chem. Phys.*, 1952, **20**, 185.
7. E. Meusel, *Chem. Ber.*, 1870, **3**, 123.
8. J. Schwiertz, A. Geist and M. Epple, *Dalton Trans.*, 2009, 2921.
9. A. Tamburini, P. Pitò, A. Cipollina, G. Micalè and M. Ciofalo, *J. Membr. Sci.*, 2013, **447**, 260.
10. J. M. Leger, A. L. Holt, and S. A. Carter, *Appl. Phys. Lett.*, 2006, **88**, 111901.
11. J.R. Ferraro and A.T. Sherren, *Inorg. Chem.*, 1978, **17**, 2498.
12. D.R. Bloomquist and R.D. Willett, *Coord. Chem. Rev.*, 1982, **47**, 125.
13. H. Yokoi, M. Sai and T. Isobe, *Chem. Lett.*, 1972, 25.
14. (a) O. M. Yaghi, M. O’Keeffe, N. W. Ockwig, H. K. Chae, M. Eddaoudi, and J. Kim, *Nature* 2003 J. M. Leger, A. L. Holt, and S. A. Carter, *Appl. Phys. Lett.*, 2006, **88**, 111901, **423**, 705. (b) S. Kitagawa, R. Kitaura and S. Noro, *Angew. Chem., Int. Ed.* 2004, **43**, 2334. (c) G. Férey, *Chem. Soc. Rev.* 2008, **37**, 191.
15. H. K. Chae, D. Y. Siberio-Perez, J. Kim, Y. Go, M. Eddaoudi, A. J. Matzger, M. O’Keeffe and O. M. Yaghi, *Nature* 2004, **427**, 523. (b) G. Férey, C. Mellot-Draznieks, C. Serre, F. Millange, J. Dutour, S. Surble and I. Margiolaki, *Science* 2005, **309**, 2040. (c) J. R. Li, J. Sculley and H. C. Zhou, *Chem. Rev.*

- 2012, **112**, 869.
16. G. Li, W. Yu, Y. Cui, *J. Am. Chem. Soc.* 2008, **130**, 4582.
17. (a) K. H. Park, K. Jang, S. U. Son and D. A. Sweigart, *J. Am. Chem. Soc.* 2006, **128**, 8740. (b) M. Banerjee, S. Das, M. Yoon, H. J. Choi, M. H. Hyun, S. M. Park, G. Seo and K. Kim, *J. Am. Chem. Soc.* 2009, **131**, 7524. (c) D. B. Dang, P. Y. Wu, C. He, Z. Xie and C. Y. Duan, *J. Am. Chem. Soc.* 2010, **132**, 14321. (d) M. Yoon, R. Srirambalaji, and K. Kim, *Chem. Rev.* 2012, **112**, 1196. (e) J. Gao, L. Bai, Q. Zhang, Y. Li, G. Rakesh, J.-M. Lee, Y. Yang, Q. Zhang, *Dalton Trans.* 2014, **43**, 2559. (f) K. Mo, Y. Yang, Y. Cui, *J. Am. Chem. Soc.* 2014, **136**, 1746.
18. (a) H. Ōkawa, A. Shigematsu, M. Sadakiyo, T. Miyagawa, K. Yoneda, M. Ohbam and H. Kitagawa, *J. Am. Chem. Soc.* 2009, **131**, 13516. (b) M. Kurmoo, *Chem. Soc. Rev.* 2009, **38**, 1353.
19. (a) R. Kitaura, K. Fujimoto, S. Noro, M. Kondo and S. Kitagawa, *Angew. Chem., Int. Ed.* 2002, **41**, 133. (b) K. Otsubo, Y. Wakabayashi, J. Ohara, S. Yamamoto, H. Matsuzaki, H. Okamoto, K. Nitta, T. Uruga and H. Kitagawa, *Nat. Mater.* 2011, **10**, 291. (c) J. Martí-Rujas, N. Islam, D. Hashizume, F. Izumi, M. Fujita, H. J. Song, H. C. Choi and M. Kawano, *Angew. Chem., Int. Ed.* 2011, **50**, 6105; (f) X. Y. Dong, B. Li, B. B. Ma, S. J. Li, M. M. Dong, Y. Y. Zhu, S. Q. Zang, Y. Song, H. W. Hou, Thomas. C. W. Mak, *J. Am. Chem. Soc.* 2013, **135**, 10214.
20. E. Y. Lee and M. P. Suh, *Angew. Chem. Int. Ed.*, 2004, **43**, 2798.
21. (a) G. Xu, J. Yao, K. Wang, L. He, P. A. Webley, C. S. Chen, H. Wang, *J. Membr. Sci.* 2011, **385-386**, 187. (b) D. Zacher, A. Baunemann, S. Hermes and R. A. Fischer, *J. Mater. Chem.* 2007, **17**, 2785. (c) M. Kubo, W. Chaikittisilp and T. Okubo, *Chem. Mater.* 2008, **20**, 2887. (d) A. Huang, H. Bux, F. Steinbach and J. Caro, *Angew. Chem., Int. Ed.* 2010, **49**, 4958. (e) G. Lu and J. T. Hupp, *J. Am. Chem. Soc.* 2010, **132**, 7832.
22. (a) J. A. Bohrman, M. A. Carreon, *Chem. Commun.* 2012, **48**, 5130. (b) Y. Pan, T. Li, G. Lestari, Z. Lai, *J. Membr. Sci.* 2012, 390-391, 93. (c) M. A. Snyder and M. Tsapatsis, *Angew. Chem., Int. Ed.* 2007, **46**, 7560.

23. (a) O. Shekhah, H. Wang, S. Kowarik, F. Schreiber, M. Paulus, M. Tolan, C. Sternemann, F. Evers, D. Zacher, R. A. Fischer and C. Wöll, *J. Am. Chem. Soc.* 2007, **129**, 15118. (b) O. Shekhah, H. Wang, M. Paradinas, C. Ocal, B. Schüpbach, A. Terfort, D. Zacher, R. A. Fischer and C. Wöll, *Nat. Mater.* 2009, **8**, 481.
24. (a) R. Ameloot, L. Stappers, J. Fransaer, L. Alaerts, B. F. Sels and D. E. De Vos, *Chem. Mater.* 2009, **21**, 2580. (b) R. Ameloot, L. Pandey, M. Van der Auweraer, L. Alaerts, B. F. Sels and D. E. De Vos, *Chem. Commun.* 2010, **45**, 3735.
25. (a) R. Makiura, S. Motoyama, Y. Umemura, H. Yamanaka, O. Sakata and H. Kitagawa, *Nat. Mater.* 2010, **9**, 565. (b) S. Motoyama, R. Makiura, O. Sakata and H. Kitagawa, *J. Am. Chem. Soc.* 2011, **133**, 5640.
26. A. Bétard, H. Bux, S. Henke, D. Zacher, J. Caro and R. A. Fischer, *Microporous Mesoporous Mater.* 2012, **150**, 76.
27. P. Horcajada, C. Serre, D. Grosso, C. Boissière, S. Perruchas, C. Sanchez and G. Férey, *Adv. Mater.* 2009, **21**, 1931.
28. H. Zhou, H. Dang, J. H. Yi, A. Nanci, A. Rochefort and J. D. Wuest, *J. Am. Chem. Soc.*, 2007, **129**, 13774.
29. Y. X. Hu, S. C. Xiang, W. W. Zhang, Z. X. Zhang, L. Wang, J. F. Bai and B. L. Chen, *Chem. Commun.*, 2009, 7551.
30. Notes: **1** and **2** showed almost the same PXRD patterns, indicating that the metal-organic framework structure is not affected by guest-exchange; as a consequence, **1** and **2** possess the same crystal structure (just guests in pores are difference between **1** and **2**).

TOC

A three-dimensional NbO-type metal-organic framework (MOF) and its thin films on α -Al₂O₃ and SiO₂ show novel reversible guest-dependent thermochromic behaviors.